



Conceptual Spacer Design for the ATR GEN I Target for Pu-238 Production in the Advanced Test Reactor at Idaho National Laboratory

May 2024

Changing the World's Energy Future

Jill R Mitchell



DISCLAIMER

This information was prepared as an account of work sponsored by an agency of the U.S. Government. Neither the U.S. Government nor any agency thereof, nor any of their employees, makes any warranty, expressed or implied, or assumes any legal liability or responsibility for the accuracy, completeness, or usefulness, of any information, apparatus, product, or process disclosed, or represents that its use would not infringe privately owned rights. References herein to any specific commercial product, process, or service by trade name, trade mark, manufacturer, or otherwise, does not necessarily constitute or imply its endorsement, recommendation, or favoring by the U.S. Government or any agency thereof. The views and opinions of authors expressed herein do not necessarily state or reflect those of the U.S. Government or any agency thereof.

Conceptual Spacer Design for the ATR GEN I Target for Pu-238 Production in the Advanced Test Reactor at Idaho National Laboratory

Jill R Mitchell

May 2024

**Idaho National Laboratory
Idaho Falls, Idaho 83415**

<http://www.inl.gov>

**Prepared for the
U.S. Department of Energy
Under DOE Idaho Operations Office
Contract DE-AC07-05ID14517**

Conceptual Spacer Design for the ATR GEN I Target for Pu-238 Production in the Advanced Test Reactor at Idaho National Laboratory

Jill Mitchell¹

¹ Idaho National Laboratory, Idaho Falls, Idaho

Primary Author Contact Information: jill.mitchell@inl.gov

[Placeholder for Digital Object Identifier (DOI) to be added by ANS]

The initial target design used for Pu-238 production at Idaho National Laboratory was designed by Oak Ridge National Laboratory to optimize the production of Pu-238 in the High Flux Isotope Reactor (HFIR) and are referred to as HFIR GEN II targets. To take advantage of the Advanced Test Reactor's (ATR) taller active core region, a re-design of the HFIR GEN II targets was needed. It was proposed to stack two HFIR GEN II targets nose to nose about the core center line; however, this resulted in excessive neutron and photon heating in the pellets located in the center. This peak heating was not desirable so three alternative designs were investigated for the ATR GEN I targets. The python-based code, MCNP to ORIGEN2 in Python (MOPY), was used to calculate the heating rates after 40 days of irradiation to capture the effects of each configuration. The purpose of this paper is to document the details of these conceptual design calculations and comparisons for the ATR GEN I targets.

I. INTRODUCTION

Qualification of multiple Advanced Test Reactor (ATR) positions for Pu-238 production has been ongoing at Idaho National Laboratory (INL) as part of the campaign to restart domestic production of plutonium-238 used in radioisotope power systems (RPS) by the National Aeronautical and Space Administration (NASA) and Department of Energy (DOE) Office of Nuclear Energy (NE), Office of Nuclear Infrastructure Program (NE-3). As part of the qualification process, multiple target designs and Np concentrations have been evaluated to support and optimize Pu-238 production in ATR.

The purpose of this paper is to document the design considerations and conceptual calculations that were required to move from a single Pu-238 production target to two Pu-238 production targets per ATR position.

II. Pu-238 PRODCUTION TARGET DESIGNS

II.A. HFIR GEN II Target

The initial target design used for Pu-238 was designed by Oak Ridge National Laboratory (ORNL) and

is referred to as the High Flux Isotope Reactor (HFIR) GEN II target.

The HFIR GEN II targets consist of a stack of fifty-two cylindrical pellets composed of 20-volume% neptunium oxide (NpO₂), 70-volume% aluminum, and 10-volume% void as well as an aluminum dummy pellet on the top and bottom of the stack up, see Fig. 1. The targets are approximately 33 inches long and centered around the core center line to optimize the production of Pu-238.

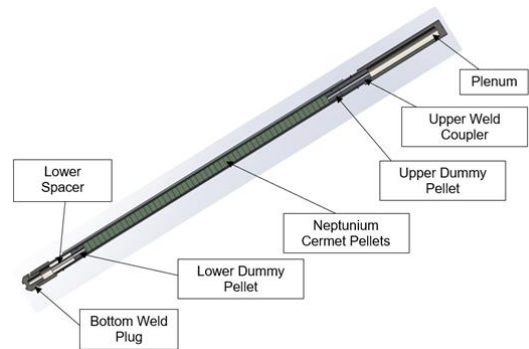


Fig. 1. Enlarged Image of HFIR GEN II Target (not to scale).

This design was initially chosen as it could interface with both HFIR and ATR and streamline the production and post irradiation processing of the targets. Due to ATR having a much larger active core region than HFIR, a single target was not an efficient use of the available production possibilities. The single target design resulted in a lower Pu-238 production than desired due to the low amount of Np pellets that could be irradiated. A new design was proposed that included reducing the height of the HFIR Gen II target and then stacking two targets nose to nose around the core center line of ATR that would make better use of ATR's core height.

II.B. ATR GEN I Target

To utilize the full height of the ATR core to increase overall Pu-238 production and still maintain a common target for both ORNL and INL irradiation it was proposed

for ATR irradiations to stack two smaller targets on top of each other and then place them into the desired ATR position. The target endpoints would be oriented around the core center line, increasing the number of pellets that can be irradiated, as shown in Fig. 2. Some adjustments were made to the overall length and internal configuration of the target. These new targets are referred to as ATR GEN I targets, as illustrated in Fig. 3. Like the HFIR Gen II targets, the ATR GEN I targets consists of a stack of cylindrical pellets, composed of 20-volume% neptunium oxide (NpO_2), 70-volume% aluminum, and 10-volume% void as well as a spacer pellet on the top of each stack. The ATR GEN I targets are approximately 28.69 inches long.

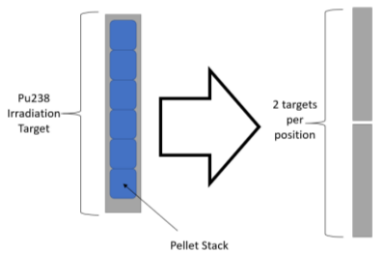


Fig. 2. ATR GEN I Target Assembly.

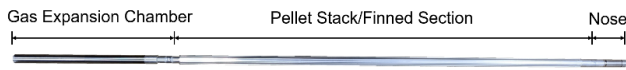


Fig. 3. ATR GEN I Target

Preliminary evaluations of stacking the two targets nose to nose showed significant neutron and gamma heating at the core center line, approximately 480 W/g after 40 days of irradiation in ATR, as shown in Fig. 4. To mitigate this peak heating, it was proposed to replace the existing Al spacers located at the top of the pellet stack with a new spacer composed of different material.

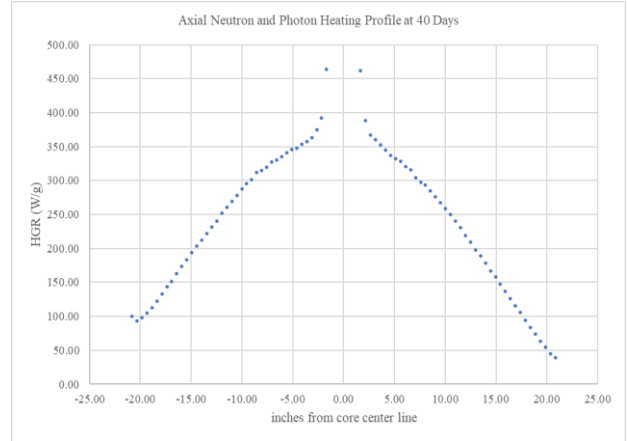


Fig. 4. Neutron and Photon heating rates after 40 days of irradiation in the SFT at 23.1 MW.

III. SPACER REQUIREMENTS

The primary requirement for the new spacer was the need to reduce the significant heating of the target ends. In addition, the following options were considered when exploring different designs. (1) The material needed to be compatible with ATR requirements and limitations. (2) The material needed to be compatible with HFIR requirements and limitations. (3) The material needed to be one that could be obtained without excessive cost, wait times, or machining.

Three material configurations were considered as possible options during the conceptual design: (1) tantalum plus stainless steel; (2) hafnium plus stainless steel; and (3) samarium plus stainless steel. These materials were placed at the top of each pellet stack and are near each other when the targets are placed nose to nose, as shown in Fig. 5. To determine if they were viable design options, heat generation rates were calculated.

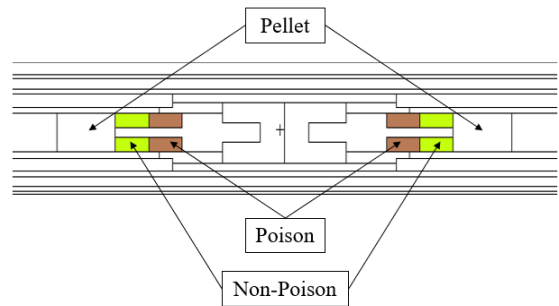


Fig. 5. Simplified MCNP model identifying the location of the spacer materials in reference to the pellet.

IV. Pu-238 NEUTRON AND PHOTON HEATING RATES

IV.A. Computer Methods & Models

The general-purpose Monte Carlo N-Particle transport code, MCNP (Ref. 1) (Ref. 2), was used to model and evaluate the ATR Gen I targets during the conceptual design. MCNP was used to calculate the neutron and photon heat generation rates within all Pu-238 experiment materials. MCNP was also used to calculate the neutron fluxes and reaction rates for pertinent reactions on the neptunium pellet material and this information was then passed into ORIGEN2 (Ref. 3) to deplete the neptunium pellet material. The ENDF/B-VII.0 cross section library (Ref. 4) was used along with the neptunium-236m cross section library obtained from TENDL-2017 (Ref. 5). The standard ATR cross section library (Ref. 7) was used for ORIGEN2 along with MCNP-calculated replacement cross sections. The python-based code, MCNP to ORIGEN2 in Python (MOPY), was used to more easily extract the fluxes and reaction rates calculated from MCNP and pass them to ORIGEN2.

The neutron and photon heating rates for the ATR Gen I target were calculated using a 3 radial, 7 axial-region fuel model of the ATR. For the purpose of this analysis, it was assumed that the targets would be located in the South Flux Trap (SFT) of the ATR, see Fig. 6. This location was chosen as the HFIR Gen II targets had previously been qualified for irradiation in ATR in the SFT.

To completely capture the rise in heating in the pellets, during the conceptual calculations, the heating rates were evaluated for multiple time-steps within 40 days of irradiation. Forty days was adequate to demonstrate the rise in pellet heating through an ATR cycle and see the impacts of the new spacer material on the heating rates.

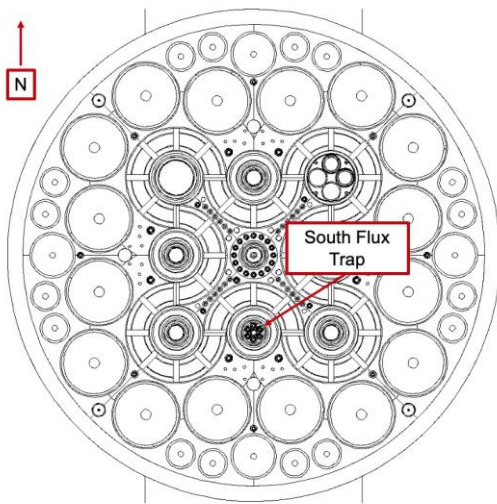


Fig. 6. MCNP cross section of ATR showing the south flux trap.

IV.B. Calculations

Each corner lobe in ATR is designed to operate individually; the core power used in calculating heat generation rates and flux must be scaled to the nearest lobe. This is done in the following fashion:

By tallying the fission energy in the driver fuel in each lobe, then summing them, the core fission energy is calculated as shown in Equation (1). The lobe power is then calculated in Equation (2) by multiplying the expected core power by the lobe energy fraction of the calculated core energy. The expected core power is the sum of all the lobe powers for a given ATR Cycle. The scaled core power is then calculated by dividing the expected lobe power by the calculated lobe and multiplying by the expected core power as shown in Equation (3).

$$\begin{aligned} & \text{Calculated Core Energy (MeV)} \\ &= \sum_i^4 \left[\text{Calculated Lobe Fuel Mass (g)}_i \right. \\ & \quad \left. \times \text{Calculated Lobe Fuel F7 Tally} \left(\frac{\text{MeV}}{\text{g}} \right)_i \right] \end{aligned} \quad (1)$$

$$\begin{aligned} & \text{Calculated Lobe Power (MW)} \\ &= \text{Expected Core Power (MW)} \\ & \quad \times \frac{\text{Calculated Lobe Energy (MeV)}}{\text{Calculated Core Energy (MeV)}} \end{aligned} \quad (2)$$

$$\begin{aligned} & \text{Scaled Core Power (MW)} \\ &= \text{Expected Core Power (MW)} \\ & \quad \times \frac{\text{Expected Lobe Power (MW)}}{\text{Calculated Lobe Power (MW)}} \end{aligned} \quad (3)$$

MCNP reports tally results normalized per source particle. The MCNP type 6 energy deposition tally results were used to calculate heat generation rates. The MCNP tally type 6 has units of MeV/g per source particle (fission neutron for prompt neutron, gamma heating, and fission heating).

The heat generation rate values (Ref. 6) are calculated using the MCNP tally type 6 results, the heating normalization factor (HNF), and the ATR core power. Prompt neutron and gamma heating rates (PHR) are calculated using equation (4).

$$\text{PHR} = (f_6)(\text{HNF})(\text{Core Power}) \frac{W}{g} \quad (4)$$

V. RESULTS

When first evaluating two ATR Gen I targets placed nose to nose in the same position, it was discovered that significant heating occurred in the center of the stack-up, as shown in Fig. 4. To reduce this heating three material configurations were considered. MCNP models were created for each material configuration and MOPY was executed to obtain the tallies needed to calculate the neutron and photon heating rates. Figures 7-9 show the heating profiles for tantalum / stainless steel, hafnium / stainless steel, and samarium / stainless steel spacers.

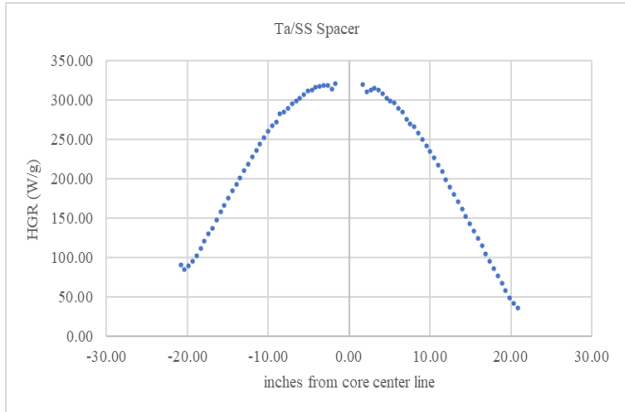


Fig. 7. Neutron and Photon heating rates in Pu-238 targets with a Tantalum /Stainless Steel spacer after 40 days of irradiation.

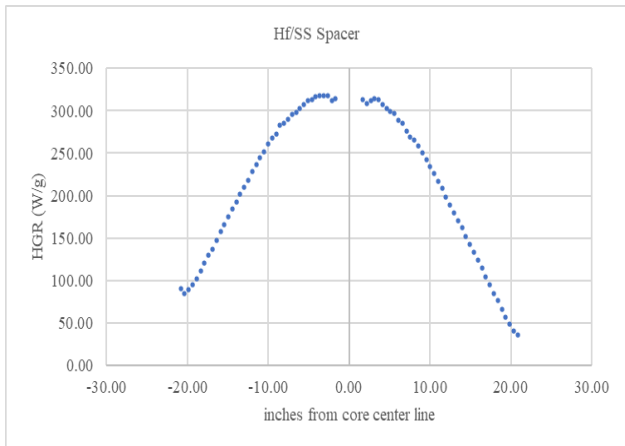


Fig. 8. Neutron and Photon heating rates in Pu-238 targets with a Hafnium /Stainless Steel spacer after 40 days of irradiation.

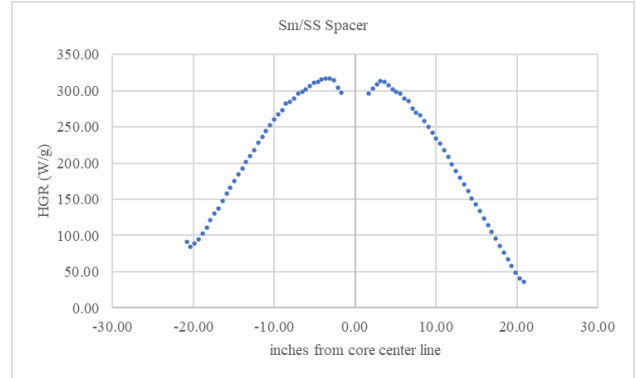


Fig. 9. Neutron and Photon heating rates in Pu-238 targets with a Samarium/Stainless Steel spacer after 40 days of irradiation.

The heating profiles showed that applying the spacers reduced the heating peaks appropriately. Tables 1-3 document the maximum and minimum heating rates in Watts/gram for each spacer configuration. Table 4 reports the percent difference that is observed when comparing each new material configuration to the original configuration. By applying the spacers, the peak heating locations moved from next to the spacer to a few pellets away.

TABLE I. Maximum and minimum neutron and photon heating rates with a tantalum/stainless steel spacer.

Neutron and Photon Heating Rates (W/g) With Ta - SS Spacer					
	BOC	10 EFPDs	20 EFPDs	30 EFPDs	40 EFPDs
max	26.39	237.10	260.95	289.24	321.44
min	8.35	27.88	29.18	32.04	35.74

TABLE II. Maximum and minimum neutron and photon heating rates with a hafnium/stainless steel spacer.

Neutron and Photon Heating Rates (W/g) With Hf - SS Spacer					
	BOC	10 EFPDs	20 EFPDs	30 EFPDs	40 EFPDs
max	26.43	237.00	260.67	287.82	317.92
min	8.35	27.88	29.18	32.04	35.74

TABLE III. Maximum and minimum neutron and photon heating rates with a samarium / stainless steel spacer.

Neutron and Photon Heating Rates (W/g) With Sm - Al Spacer					
	BOC	10 EFPDs	20 EFPDs	30 EFPDs	40 EFPDs
max	26.97	236.27	259.63	286.81	316.72
min	8.35	27.88	29.18	32.04	35.73

TABLE IV. Percent difference between peak heating for different spacer configurations.

Spacer Configuration	% difference
original spacer	--
Ta-SS	39.6%
Hf-SS	40.6%
Sm-SS	41.0%

VI. CONCLUSIONS

Pu-238 production at INL is ongoing using ORNL manufactured targets, which are referred to as PFS ATR Generation I Targets. To mitigate the peak heating that was calculated when stacking two targets nose to nose, three spacer configurations were evaluated using the python-based code, MCNP to ORIGEN2 in Python (MOPY). MOPY was used to specifically look at the neutron and photon heat generation rates for each spacer configuration.

Analysis showed that all three configurations, tantalum/stainless steel, hafnium/stainless steel, and samarium/stainless steel significantly reduced the peak heating with the samarium configuration showing the greatest reduction. Due to the lower heating and additional program requirements, the samarium/stainless steel spacer was recommended as part of the conceptual design to irradiate the ATR Gen I targets. As a follow-up to this conceptual analysis and in moving to the next phase of the ATR Gen I qualification, it was determined that a samarium/aluminum spacer provided the best configuration to reduce the neutron and photon heat generation rates.

ACKNOWLEDGMENTS

This work was funded by NASA Interagency Agreement # NNH19OB05A and DOE contract DE-AC05-00OR22725 and DE-AC07-05ID14517.

This work also leveraged the High-Performance Computing Center at Idaho National Laboratory, which is supported by the Office of Nuclear Energy of the U.S. Department of Energy and the Nuclear Science User Facilities under Contract No. DE-AC07-05ID14517.

REFERENCES

1. F. Brown, B. Kiedrowsky, et. al, "MCNP5-1.60 Release Notes," LA-UR-10-06235 (2010).
2. X-5 Monte Carlo Team, "MCNP-A General Monte Carlo N-Particle Transport Code, Version 5," Volume I, LA-UR-03-1987, Los Alamos National Laboratory, April 24, 2003 (Revised 10/3/05) and Volume II, LA-CP-03-0245, Los Alamos National Laboratory, April 24, 2003 (Revised 10/3/05) (Vol. II is available with a licensed copy of MCNP).
3. A. G. Croff, "ORIGEN 2: A Versatile Computer Code for Calculating the Nuclide Compositions and Characteristics of Nuclear Materials, Nuclear Technology," Vol. 62, pp. 335-352, 1983.
4. M.B. Chadwich et al., October 2006. "ENDF/B-VII.0: Next Generation Evaluated Nuclear Data Library for Nuclear Science and Technology," UCRL-JRNL-225066,
5. TENDL-2017, "A.J. Koning and D. Rochman, "Modern Nuclear Data Evaluation With The TALYS Code System", Nuclear Data Sheets 113 (2012) 2841.
6. GDE-594, "Experiment Design and Analysis Guide – Neutronics & Physics," Rev. 2, (Internal Report) January 11, 2017.
7. B. G. Schnitzler, BGS-6-91, "Origen2 Cross Section Library Assessment for ATR Applications", (Internal Report), Idaho National Laboratory, April 1991.
8. "Experiment Analysis Documentation / MOPY", (Internal Report), Idaho National Laboratory, January 2022.